Many-Body Dynamics in Monitored Atomic Gases without Postselection Barrier

Gianluca Passarelli,[1,*,†] Xhek Turkeshi,[2,*] Angelo Russomanno,[3] Procolo Lucignano,[4] Marco Schirò,[2] and Rosario Fazio[5,4]

[1]*CNR-SPIN, c/o Complesso di Monte S. Angelo, via Cinthia—80126—Napoli, Italy*
[2]*JEIP, UAR 3573 CNRS, Collège de France, PSL Research University, 75321 Paris Cedex 05, France*
[3]*Scuola Superiore Meridionale, Università di Napoli Federico II, I-80138 Napoli, Italy*
[4]*Dipartimento di Fisica, Università di Napoli Federico II, I-80126 Napoli, Italy*
[5]*The Abdus Salam International Center for Theoretical Physics, 34151 Trieste, Italy*

(Received 13 June 2023; revised 11 September 2023; accepted 14 March 2024; published 15 April 2024)

We study the properties of a monitored ensemble of atoms driven by a laser field and in the presence of collective decay. The properties of the quantum trajectories describing the atomic cloud drastically depend on the monitoring protocol and are distinct from those of the average density matrix. By varying the strength of the external drive, a measurement-induced phase transition occurs separating two phases with entanglement entropy scaling subextensively with the system size. Incidentally, the critical point coincides with the superradiance transition of the trajectory-averaged dynamics. Our setup is implementable in current light-matter interaction devices, and most notably, the monitored dynamics is free from the postselection measurement problem, even in the case of imperfect monitoring.

DOI: 10.1103/PhysRevLett.132.163401

Introduction.—When a quantum system is externally measured, its dynamic is strongly altered. The decay of an atom, for example, will occur through a sudden quantum jump from the excited to the ground state at a random time. The evolution of quantum systems along chosen trajectories has been intensively investigated for almost forty years [1–3]. Only very recently, however, monitored dynamics entered the world of many-body systems. Two independent works [4,5] showed that a quantum many-body system subject to a mixed evolution composed of unitary intervals interrupted by local measurements undergoes a transition in its quantum correlation pattern which is invisible to the properties of the average density matrix. Only by resolving the dynamics along each trajectory is it possible to construct nonlinear functions of quantum states, such as entanglement measures or trajectory correlations, able to reveal these so-called measurement-induced phase transitions (MIPT). An extensive research activity followed these initial works [6–8], analyzing salient aspects of measurement-induced phases in monitored quantum circuits [9–22], noninteracting [23–38] and interacting [39–44] monitored Hamiltonian systems. Common to these frameworks is the variety of entanglement patterns induced by measurements, that are deeply tied to the encoding-decoding properties of quantum channels [45–55].

Despite this large theoretical effort, the experimental evidence of MIPTs is much more limited with only three pioneering experimental works at present [56–58]. Following a first quantum simulation with trapped ions [56] the scaling close to the critical point has been explored with the IBM quantum processor [57]. A fundamental reason hinders the possibility of observing monitored phases, known as the postselection problem. To perform averages of observables along a given trajectory, one should reproduce the same sequence of random jumps with sufficient probability. This task is challenging as the probability of reproducing the same trajectory scales to zero exponentially with system size and timescale, explaining why experiments were limited to a few sites and the considerable efforts required to increase the lattice length. The postselection barrier can be avoided by quantum-classical approaches that combine measurement outcomes to classical postprocessing [45,59–61]. These methods however require a perfect detection and the ability to efficiently simulate the quantum dynamics on a classical computer. In certain quantum circuits, postselection overhead can be mitigated by resorting to space-time duality [58,62,63]. Another approach was proposed in adaptive quantum circuits [64,65], where the measurement registry conditions the evolution so as to render MIPTs visible in the average dynamics (at density matrix level). However, this route generally fails as feedback may alter the physics of the system, and separate transitions may occur in the monitored and average dynamics [66–69]. The postselection problem remains a formidable hurdle to overcome, and the search for cases where it can be mitigated is necessary for experimental progress in monitoring quantum many-body systems.

Here we show that there is a class of infinite-range spin systems where monitored many-body dynamics can be efficiently realized with a postselection overhead growing, at most, *polynomially* with the system size. These systems

have a nontrivial monitored dynamics, which is yet experimentally accessible in atomic ensembles driven by a laser field and in the presence of a collective decay. Here, the type of measurement is pivotal in determining the entanglement behavior of the quantum trajectories describing the system. Different monitoring protocols lead to a different scaling of entanglement measures throughout the phase diagram, highlighting the measurement-induced nature of the system. The quantum trajectories describing the system undergo a MIPT separating two subvolume law behaviors. Incidentally, this measurement-induced criticality coincides with the dissipative (in this case, superradiant) transition of the average dynamics, a possibility already discussed in the literature [42,66–69]. As in these cases, critical and off-critical features of the dissipative and monitoring-induced phases are generally inequivalent, as the mechanism underpinning these phenomena is different. (We have further discussed this fact in the Supplemental Material [70] with a concrete example having a phase transition at the average level, but lacking a MIPT.).

The system consists of a cloud of N atoms (each behaving as a two-level system with associated Pauli matrices $\hat{\sigma}_i^\alpha$, $\alpha = x, y, z$ for the ith atom), driven by an external laser with collective decay [78]. In the absence of monitoring, its density matrix obeys the Lindblad equation

$$\dot{\hat{\rho}} = \mathcal{L}(\hat{\rho}) \equiv -i[\hat{\mathcal{H}}, \hat{\rho}] + \frac{\kappa}{J}\left(\hat{J}_- \hat{\rho} \hat{J}_+ - \frac{1}{2}\{\hat{J}_+ \hat{J}_-, \hat{\rho}\}\right), \tag{1}$$

where $\hat{J}_\alpha = \sum_i \hat{\sigma}_i^\alpha/2$, $\hat{J}_\pm = \hat{J}_x \pm i\hat{J}_y$, $J = N/2$ is the total spin, and $\hat{\mathcal{H}} = \omega_0 \hat{J}_x$. The steady state has a superradiant phase transition separating a normal from a time-crystal phase [79–81]. The dynamic governed by (1) was recently realized experimentally [78]. Following the evolution along a quantum trajectory, i.e., unraveling (1), requires specifying a monitoring protocol [82,83]. As we detail below, although the average dynamics is the same [cf. (1)], different types of measurements generate inequivalent trajectory ensembles, a fact already noted in, e.g., [32,33,35]. Their distinct traits are showcased in any nonlinear function of the state, e.g., in entanglement measures. We will separately discuss two, experimentally motivated, monitoring protocols. The system is either coupled to a photodetector, where measurement acts as quantum jumps (QJ), or to a homodyne detector, continuously probing the system and leading to a quantum state diffusion (QSD). We quantify the entanglement in the fluctuating steady state through entanglement entropy and quantum Fisher information.

Quantum jumps.—In this case, the system evolves according to an (smooth) effective non-Hermitian Hamiltonian $\hat{\mathcal{H}}_{\rm nj} = \hat{\mathcal{H}} - i(\kappa/2J)\hat{J}_+\hat{J}_-$, interrupted, at random times, by quantum jumps when the wave function $|\psi(t)\rangle$ changes abruptly as

$$|\psi(t_+)\rangle = \frac{\hat{J}_-|\psi(t_-)\rangle}{\sqrt{\langle\psi(t_-)|\hat{J}_+\hat{J}_-|\psi(t_-)\rangle}}. \tag{2}$$

In a time interval δt, jumps occur with a probability $\delta p = \kappa\delta t\langle\hat{J}_+\hat{J}_-\rangle/J$. Details of the numerics are given in the Supplemental Material [70].

The QJ unraveling leads to a ensemble of stochastic trajectories fixed by the occurrence (time) of the jumps. The Lindblad evolution (1) describes the average features of this ensemble [2], but does not capture its higher cumulants. These features are probed by nonlinear functions of the state, e.g., the entanglement measures considered in this manuscript [84].

We first consider the entanglement entropy, defined for a pure state $|\psi(t)\rangle$ and a bipartition of the system into two sets A and B, by $S_A(|\psi(t)\rangle) = -\mathrm{Tr}_A(\hat{\rho}_A \ln \hat{\rho}_A)$. Here, $\hat{\rho}_A = \mathrm{Tr}_B|\psi(t)\rangle\langle\psi(t)|$ is the partial trace over the degrees of freedom of subsystem B. We will consider balanced partitions with $N_A = N_B = N/2$, and the entanglement entropy at long times is then averaged over the quantum trajectories and over the time domain $\overline{S_{N/2}}$.

In the evolution dictated by (2), quantum correlations are built by collective jumps, and the external drive leads to phase shifts between different components of the quantum state. Their interplay leads to a nontrivial behavior of the entanglement for quantum trajectories. In Fig. 1(a), we plot the averaged entropy $\overline{S_{N/2}}$ as a function of ω_0/κ for several values of N. In the small ω_0 regime, the entanglement entropy is essentially independent of N: The system is in an area-law phase. An anomaly develops near $\omega_0/\kappa \sim 1$. The singularity is clearly visible in the inset of Fig. 1(a). The derivative of $\overline{S_{N/2}}$ has a logarithmic divergence of the peak height with N. The MIPT coincides with the superradiant transition of the average state, separating a normal from a time-crystal phase [79]. This incidental fact [85], will *not* be used in the following, as the average density matrix does not reveal the entanglement properties of the trajectory. At the critical point, the entanglement diverges logarithmically as shown in Fig. 1(b). For $\omega_0/\kappa > 1$ the entropy grows more slowly with N. From the numerics, a good fit is obtained with $\overline{S_{N/2}} \sim \ln^\beta N$ with a nonuniversal exponent $\beta < 1$ that decreases moving away from the transition. In the limit $\omega_0/\kappa \gg 1$, β tends to zero. A more careful inspection based on of Figs. 1(c) and 1(d) suggests $\overline{S_{N/2}} \sim \ln\ln N$. The entropy grows as $\ln t$ up to a saturation time that depends logarithmically on N. Subextensive phases in long-range circuits have been discussed in [86–91].

It is important to estimate the overhead that we should expect from the unavoidable postselection in a brute-force experiment. The system analyzed here is free from the postselection problem. Because of the collective nature of the jumps, a quantum trajectory can be represented as a

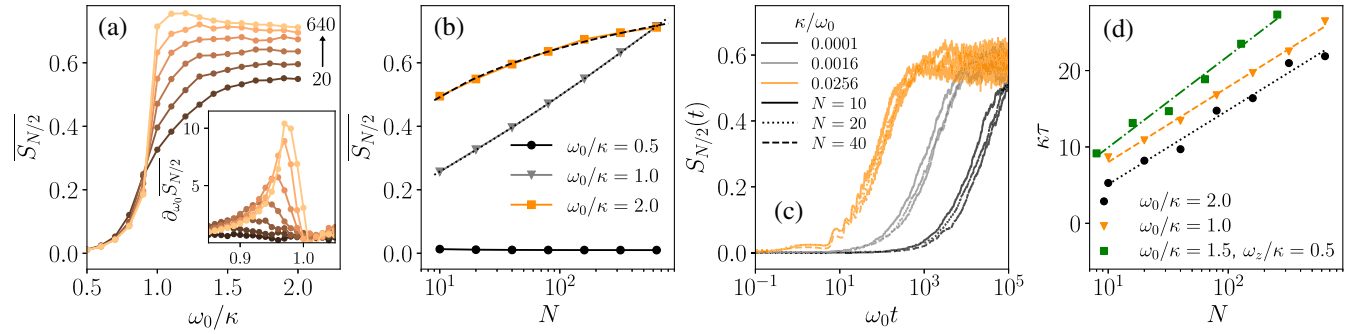

FIG. 1. Results of QJ simulations. (a) Long-time average of the half-chain entanglement entropy $\overline{S_{N/2}}$ as a function of ω_0/κ, for system sizes $N = 20, 40, 80, 160, 320, 640$. Inset: the numerical derivative of the long-time averaged entanglement entropy highlights the critical point; the peak height grows logarithmically with N. (b) Scaling of $\overline{S_{N/2}}$ as a function of N at fixed values of ω_0/κ. At the critical point, the long-time averaged entanglement entropy grows logarithmically with N (gray triangles). In the phase $\omega_0/\kappa < 1$ the behavior is area law (black circles). The scaling in the region $\omega_0/\kappa > 1$ is sublogarithmic (orange squares). Numerically, one can fit the curves as $\overline{S_{N/2}} \sim \ln^\beta N$ with a nonuniversal exponent $\beta < 1$ ($\beta \sim 0.2$ at $\omega_0/\kappa = 2$). The exponent decreases when moving away from the critical point. (c) Long-time dynamics of the entanglement entropy for several system sizes and several values of κ/ω_0. The entanglement entropy grows as $\ln t$ before saturating. (d) Dependence of the saturation time on the system size N (in all cases, $\tau \sim \ln N$).

binary string with a record of the sequence of jumps (once a time bin has been fixed). The probability of generating the same trajectory thus scales as $2^{-\tau}$ with τ of the order of the saturation time. For $\omega_0/\kappa < 1$, τ is independent on N [70]. In the subextensive regime $\omega_0/\kappa > 1$ and at the critical point $\omega_0/\kappa = 1$, the saturation time grows logarithmically with the system size,

$$\tau \sim a \log N + b; \tag{3}$$

see Fig. 1(d) (a, b constants depending on ω_0/κ). The logarithmic scaling of the saturation time is a signature of collective dissipation [71], and can be estimated from the imaginary part of the non-Hermitian Hamiltonian [70].

Combining the behavior of τ discussed above, it is straightforward to conclude that the probability of occurrence of a given trajectory is, at most, decaying as power law $N^{-\gamma}$ (with γ weakly dependent on the coupling constants). The monitored dynamic of the system we consider is thus free from the postselection problem.

This property holds for a class of long-range interacting spin systems with collective decay. We added an all-to-all term to the Hamiltonian of the form $\hat{\mathcal{H}}_z = \omega_z \hat{J}_z^2$, and the scaling of the saturation time, shown in Fig. 1(d) green squares, is still logarithmic with the system size. We also considered the case of power-law decay exchange interaction among the spins. In this case, due to the absence of permutational invariance, we can consider much more modest system sizes. The results are reported in the Supplemental Material [70]: As long as the interaction is sufficiently long range the dynamics remains postselection-free up to long times.

Quantum state diffusion.—After discussing the quantum jump evolution induced in the atomic cloud by the photodetector, we now consider the *inequivalent* quantum state diffusion dynamics induced by a (nonideal) homodyne detector [3,92]. The dynamics is given by [2]

$$d\hat{\rho}_{\rm w} = \mathcal{L}(\hat{\rho}_{\rm w}) + \sqrt{\frac{\kappa\eta}{J}} dW (\hat{J}_- \hat{\rho}_{\rm w} + \hat{\rho}_{\rm w} \hat{J}_+ - 2\langle \hat{J}_x \rangle \hat{\rho}_{\rm w}), \tag{4}$$

where dW is a Gaussian Îto noise with $\overline{dW} = 0$ and $dW^2 = dt$. In Eq. (4) we have introduced the detector efficiency $\eta \in [0, 1]$ to treat the effect of noise: $\eta = 1$ corresponds to a perfect detector, and $\eta < 1$ describe imperfect detection, with the limit $\eta = 0$ implying no trajectory resolution. Equation (4) provides a different unraveling of the Lindblad equation in Eq. (1) since $\hat{\rho} = \overline{\hat{\rho}_{\rm w}}$, and describes a system coupled to a homodyne detector, a framework of experimental relevance in current platforms [93]. Crucially, the homodyne current

$$dI_t = \frac{\kappa}{J} \langle \hat{J}_x \rangle + \sqrt{\frac{\kappa\eta}{J}} dW \tag{5}$$

is experimentally detectable, thus allowing for an efficient monitoring (see below). When $\eta = 1$ the monitoring is perfect; the purity of an initial state is preserved in the dynamic. In this case, the entanglement entropy is a sensitive measure of quantum correlations in the system. In Fig. 2(a) we present the average entanglement entropy varying ω_0/κ and for various system sizes. For $\omega_0 < \kappa$ the entanglement behaves qualitatively as for the quantum jump evolution [cf. Fig. 1(a)]. Differently, for $\omega_0 > \kappa$ the available system sizes show a saturation, hence an area-law phase. This is not surprising: The quantum state diffusion is a different unraveling of the Lindblad equation, Eq. (1), that is more prone to destroy entanglement, i.e., the infinite click limit of the quantum jump evolution. Remarkably, the

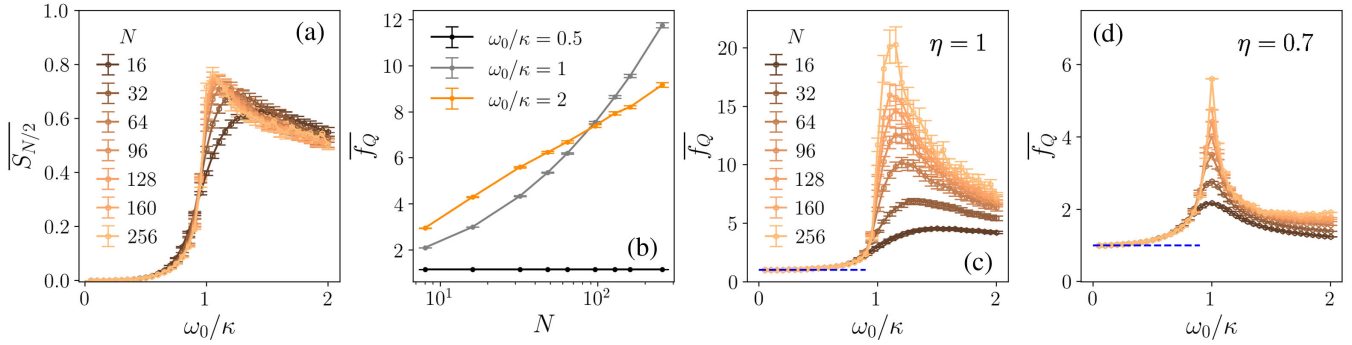

FIG. 2. Results of QSD simulations. (a) Long-time averaged entanglement entropy $\overline{S_{N/2}}$ as a function of ω_0/κ for various system sizes N. The entanglement develops a peak at the critical point $\omega_0 = \kappa$. (b) Scaling of $\overline{f_Q} = \overline{F_Q}/N$ as a function of N at the fixed values of ω_0/κ. At the critical point, the long-time averaged Fisher density grows $\propto \sqrt{N}$ (gray line). In the phase $\omega_0 < \kappa$, $\overline{f_Q}$ saturates to the constant 1 (black line). For $\omega_0 > \kappa$, the Fisher density scales logarithmically with the system size. Therefore, the system is multipartite entangled at the critical point and in the nontrivial phase. As discussed in the text, we compare the Fisher density for (c) efficient ($\eta = 0$) and (d) inefficient detectors ($\eta = 0.7$). The blue-dashed line is the constant value $\overline{f_Q} = 1$. While quantitative changes are present, the qualitative features of the phase diagram are preserved.

phase transition occurs still at $\omega_0 = \kappa$, where $\overline{S_{N/2}}$ develops a peak.

Realistic experiments have $\eta < 1$ due to decoherence to the environment, and Eq. (4) leads to mixed states, potentially altering the entanglement properties of the state [94–98]. For instance, the von Neumann entropy is not an entanglement measure in this situation, as it also embodies classical correlations. Therefore, to compare perfect and imperfect detectors, we study the quantum Fisher information (QFI), a measure of multipartite entanglement valid for pure and mixed states [99–105]. The quantum Fisher information is $F_Q(\hat{\rho}_w) = \max \text{eigval}(M)$ where the matrix $M_{\alpha,\beta} = 2\sum_{k,l} \Lambda_{k,l}\langle k|\hat{J}_\alpha|l\rangle\langle l|\hat{J}_\beta|k\rangle$ is defined for the decomposition $\hat{\rho}_w = \sum_k \lambda_k |k\rangle\langle k|$ and $\Lambda_{k,l} = (\lambda_k - \lambda_l)^2/(\lambda_k + \lambda_l)$ [106]. The QFI gives a bound to the multipartite entanglement entropy: If the Fisher density $f_Q \equiv F_Q/N$ is (strictly) larger than some divider k of L, then the state contains entanglement between $(k+1)$ parties. The QFI is nonlinear in the density matrix; hence $\overline{F_Q(\hat{\rho}_w)} \neq F_Q(\overline{\hat{\rho}_w})$. We first discuss the average QFI density $\overline{f_Q}$ in the limit $\eta = 1$. In Fig. 2(b) we show the system size scaling of $\overline{f_Q}$ in the normal phase, critical point, and boundary time crystal phase. In the former, the Fisher density saturates to the constant, signaling that the system is close to a product state. For $\omega_0 > \kappa$ the Fisher density presents a logarithmic scaling with N [70]. It follows that this phase exhibits area-law entanglement and logarithmic multipartite entanglement [107]. At the critical point, a polynomial fit shows that $\overline{f_Q} \sim N^{1/2}$ [108]. In Fig. 2(c) we summarize the behavior of the Fisher density for a perfect detector ($\eta = 1$). The salient points of the above discussion are robust against noisy contribution. In Fig. 2(d) we show that the phases and the peak of $\overline{f_Q}$ at the critical point are qualitatively unaltered for efficiency rate $\eta = 0.7$. Further decreasing η we would get close to the Lindblad framework, Eq. (1), where the QFI has been computed in [109,110]. The analysis presented above shows that experimental detection is feasible in the atomic systems of interest. In the next section, we discuss in more detail an experimental implementation based on driven atomic gases and one on homodyne detection.

Experimental implementation.—The model under study here has been recently realized in trapped atomic gases coupled to a mode of the free space electromagnetic environment [78,111]. In the subwavelength regime, a fraction of the atoms share the same diffraction mode and experience a collective decay, as described by the jump operator in Eq. (2). The effective atom number can be tuned in the experiment by changing the geometry of the setup [78]. In a single-shot experiment the number of emitted photons in two orthogonal directions is measured, giving access to the quantum jumps and their statistics. In particular, by monitoring the intensity of the light emitted in the direction perpendicular to the cloud it is possible to access the population of the atomic excited states, $\langle \hat{J}_z \rangle$, and its statistics. The polynomial cost of postselection in this system suggests that reconstructing the trajectory histogram of this observable could be doable as in experiments with single qubits [112,113]. In Fig. 3(a), we compute the variance of the collective spin magnetization, showing a sharp transition at $\omega_0/\kappa = 1$. An even more direct signature of the transition can be obtained by performing homodyne detection and measuring the variance of the homodyne current $\overline{dI_t^2} \sim \overline{\langle \hat{J}_x \rangle^2}$; cf. Eq. (5). Hence from the first two moments of dI_t we can reconstruct the variance of $\langle \hat{J}_x \rangle$; cf. Fig. 3(b). *En passant*, we note that these variances constitute a lower bound of the quantum Fisher information [100]; thus they partially access multipartite entanglement aspects [114]. Collective dissipative processes such as those at play here can be engineered in other platforms

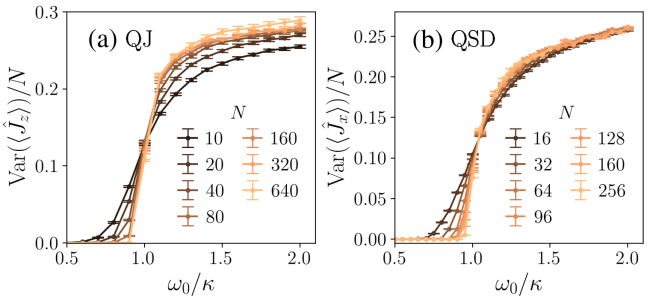

FIG. 3. (a) Rescaled trajectory variance of $\langle \hat{J}_z \rangle$ for various system sizes and along the phase diagram for the quantum jump evolution. The trajectory histogram of $\langle \hat{J}_z \rangle$ is experimentally observable; cf. Ref. [78]. (b) Rescaled trajectory variance of $\langle \hat{J}_x \rangle$ for the quantum state diffusion. This quantity is directly obtainable from the homodyne current [2].

such as atoms coupled to a cavity mode [115] or qubits collectively coupled to a microwave resonator [116] or a waveguide [117]. Similar phenomenology is expected also in other dissipative time crystals models, e.g., in [118].

Conclusions.—In this Letter, we discussed a class of many-body system where it is possible to follow the dynamics along quantum trajectories without suffering from the postselection problem. Specifically we discussed a case, that can be observed in existing experimental platforms [78,93], and studied its entanglement properties. We expect this behavior is generic in semiclassical dynamics. When the latter breaks down, we expect the postselection overhead to become again exponential.

We would like to thank M. Dalmonte, F. Iemini, P. Sierant, S. Pappalardi, G. Fux, and Z. Li for very fruitful conversations and collaborations on related topics. We acknowledge computational resources on the Collège de France IPH cluster, the CINECA award under the ISCRA initiative (IsB28_GAMING and IsCb0_QUJENU), and from MUR, PON "Ricerca e Innovazione 2014-2020," under Grant No. PIR01_00011—(I.Bi.S.Co.). This work was supported by the ANR Grant "NonEQuMat" (No. ANR-19-CE47-0001) (X. T. and M. S.), by a Google Quantum Research Award (R. F.), by PNRR MUR Project No. PE0000023-NQSTI (P. L., G. P., A. R., and R. F.), by the European Union's Horizon 2020 research and innovation program under Grant Agreement No. 101017733, by the MUR Project No. CN_00000013-ICSC (P. L.), and by the QuantERA II Programme STAQS project that has received funding from the European Union's Horizon 2020 research and innovation program under Grant Agreement No. 101017733 (P. L.). This work is cofunded by the European Union (ERC, RAVE, 101053159) (R. F).

The views and opinions expressed are however those of the author(s) only and do not necessarily reflect those of the European Union or the European Research Council. Neither the European Union nor the granting authority can be held responsible for them.

*These authors contributed equally to this work.
†Present address: Dipartimento di Fisica "E. Pancini," Università di Napoli Federico II, Monte S. Angelo, I-80126 Napoli, Italy.

[1] H. Carmichael, *Statistical Methods in Quantum Optics 1* (Springer Science & Business Media, Berlin, Germany, 1999).
[2] H. M. Wiseman and G. J. Milburn, *Quantum Measurement and Control* (Cambridge University Press, Cambridge, England, 2009).
[3] K. Jacobs, *Quantum Measurement Theory and its Applications* (Cambridge University Press, Cambridge, England, 2014).
[4] Y. Li, X. Chen, and M. P. A. Fisher, Phys. Rev. B **98**, 205136 (2018).
[5] B. Skinner, J. Ruhman, and A. Nahum, Phys. Rev. X **9**, 031009 (2019).
[6] M. P. Fisher, V. Khemani, A. Nahum, and S. Vijay, Annu. Rev. Condens. Matter Phys. **14**, 335 (2023).
[7] A. C. Potter and R. Vasseur, *Quantum Sciences and Technology* (Springer, Cham, 2022), p. 211.
[8] O. Lunt, J. Richter, and A. Pal, *Quantum Sciences and Technology* (Springer, Cham, 2022), p. 251.
[9] Y. Li, X. Chen, and M. P. A. Fisher, Phys. Rev. B **100**, 134306 (2019).
[10] M. Szyniszewski, A. Romito, and H. Schomerus, Phys. Rev. B **100**, 064204 (2019).
[11] C.-M. Jian, Y.-Z. You, R. Vasseur, and A. W. W. Ludwig, Phys. Rev. B **101**, 104302 (2020).
[12] Y. Li, R. Vasseur, M. P. A. Fisher, and A. W. W. Ludwig, arXiv:2110.02988.
[13] A. Zabalo, M. J. Gullans, J. H. Wilson, S. Gopalakrishnan, D. A. Huse, and J. H. Pixley, Phys. Rev. B **101**, 060301(R) (2020).
[14] M. Szyniszewski, A. Romito, and H. Schomerus, Phys. Rev. Lett. **125**, 210602 (2020).
[15] X. Turkeshi, R. Fazio, and M. Dalmonte, Phys. Rev. B **102**, 014315 (2020).
[16] O. Lunt, M. Szyniszewski, and A. Pal, Phys. Rev. B **104**, 155111 (2021).
[17] P. Sierant, M. Schirò, M. Lewenstein, and X. Turkeshi, Phys. Rev. B **106**, 214316 (2022).
[18] A. Nahum, S. Roy, B. Skinner, and J. Ruhman, PRX Quantum **2**, 010352 (2021).
[19] A. Zabalo, M. J. Gullans, J. H. Wilson, R. Vasseur, A. W. W. Ludwig, S. Gopalakrishnan, D. A. Huse, and J. H. Pixley, Phys. Rev. Lett. **128**, 050602 (2022).
[20] P. Sierant and X. Turkeshi, Phys. Rev. Lett. **128**, 130605 (2022).
[21] G. Chiriacò, M. Tsitsishvili, D. Poletti, R. Fazio, and M. Dalmonte, Phys. Rev. B **108**, 075151 (2023).
[22] K. Klocke and M. Buchhold, Phys. Rev. X **13**, 041028 (2023).
[23] X. Cao, A. Tilloy, and A. De Luca, SciPost Phys. **7**, 024 (2019).
[24] A. Nahum and B. Skinner, Phys. Rev. Res. **2**, 023288 (2020).
[25] M. Buchhold, Y. Minoguchi, A. Altland, and S. Diehl, Phys. Rev. X **11**, 041004 (2021).

[26] C.-M. Jian, B. Bauer, A. Keselman, and A. W. W. Ludwig, Phys. Rev. B **106**, 134206 (2022).
[27] M. Coppola, E. Tirrito, D. Karevski, and M. Collura, Phys. Rev. B **105**, 094303 (2022).
[28] M. Fava, L. Piroli, T. Swann, D. Bernard, and A. Nahum, Phys. Rev. X **13**, 041045 (2023).
[29] I. Poboiko, P. Pöpperl, I. V. Gornyi, and A. D. Mirlin, Phys. Rev. X **13**, 041046 (2023).
[30] C.-M. Jian, H. Shapourian, B. Bauer, and A. W. W. Ludwig, arXiv:2302.09094.
[31] J. Merritt and L. Fidkowski, Phys. Rev. B **107**, 064303 (2023).
[32] O. Alberton, M. Buchhold, and S. Diehl, Phys. Rev. Lett. **126**, 170602 (2021).
[33] X. Turkeshi, A. Biella, R. Fazio, M. Dalmonte, and M. Schiró, Phys. Rev. B **103**, 224210 (2021).
[34] X. Turkeshi, M. Dalmonte, R. Fazio, and M. Schirò, Phys. Rev. B **105**, L241114 (2022).
[35] G. Piccitto, A. Russomanno, and D. Rossini, Phys. Rev. B **105**, 064305 (2022).
[36] G. Piccitto, A. Russomanno, and D. Rossini, SciPost Phys. Core **6**, 078 (2023).
[37] E. Tirrito, A. Santini, R. Fazio, and M. Collura, SciPost Phys. **15**, 096 (2023).
[38] A. Paviglianiti and A. Silva, Phys. Rev. B **108**, 184302 (2023).
[39] D. Rossini and E. Vicari, Phys. Rev. B **102**, 035119 (2020).
[40] Q. Tang and W. Zhu, Phys. Rev. Res. **2**, 013022 (2020).
[41] Y. Fuji and Y. Ashida, Phys. Rev. B **102**, 054302 (2020).
[42] P. Sierant, G. Chiriacò, F. M. Surace, S. Sharma, X. Turkeshi, M. Dalmonte, R. Fazio, and G. Pagano, Quantum **6**, 638 (2022).
[43] E. V. H. Doggen, Y. Gefen, I. V. Gornyi, A. D. Mirlin, and D. G. Polyakov, Phys. Rev. Res. **4**, 023146 (2022).
[44] A. Altland, M. Buchhold, S. Diehl, and T. Micklitz, Phys. Rev. Res. **4**, L022066 (2022).
[45] M. J. Gullans and D. A. Huse, Phys. Rev. Lett. **125**, 070606 (2020).
[46] M. J. Gullans and D. A. Huse, Phys. Rev. X **10**, 041020 (2020).
[47] H. Lóio, A. De Luca, J. De Nardis, and X. Turkeshi, Phys. Rev. B **108**, L020306 (2023).
[48] S. Choi, Y. Bao, X.-L. Qi, and E. Altman, Phys. Rev. Lett. **125**, 030505 (2020).
[49] Y. Bao, S. Choi, and E. Altman, Phys. Rev. B **101**, 104301 (2020).
[50] Y. Bao, S. Choi, and E. Altman, Ann. Phys. (Amsterdam) **435**, 168618 (2021).
[51] L. Fidkowski, J. Haah, and M. B. Hastings, Quantum **5**, 382 (2021).
[52] Y. Bao, M. Block, and E. Altman, Phys. Rev. Lett. **132**, 030401 (2024).
[53] F. Barratt, U. Agrawal, A. C. Potter, S. Gopalakrishnan, and R. Vasseur, Phys. Rev. Lett. **129**, 200602 (2022).
[54] H. Dehghani, A. Lavasani, M. Hafezi, and M. J. Gullans, Nat. Commun. **14**, 2918 (2023).
[55] S. P. Kelly, U. Poschinger, F. Schmidt-Kaler, M. P. A. Fisher, and J. Marino, SciPost Phys. **15**, 250 (2023).
[56] C. Noel, P. Niroula, D. Zhu, A. Risinger, L. Egan, D. Biswas, M. Cetina, A. V. Gorshkov, M. J. Gullans, D. A. Huse, and C. Monroe, Nat. Phys. **18**, 760 (2022).
[57] J. M. Koh, S.-N. Sun, M. Motta, and A. J. Minnich, Nat. Phys. **19**, 1314 (2023).
[58] J. C. Hoke *et al.*, Nature (London) **622**, 481 (2023).
[59] Y. Li, Y. Zou, P. Glorioso, E. Altman, and M. P. A. Fisher, Phys. Rev. Lett. **130**, 220404 (2023).
[60] Y. Li and M. P. A. Fisher, Phys. Rev. B **108**, 214302 (2023).
[61] S. J. Garratt and E. Altman, arXiv:2305.20092.
[62] M. Ippoliti and V. Khemani, Phys. Rev. Lett. **126**, 060501 (2021).
[63] T.-C. Lu and T. Grover, PRX Quantum **2**, 040319 (2021).
[64] T. Iadecola, S. Ganeshan, J. H. Pixley, and J. H. Wilson, Phys. Rev. Lett. **131**, 060403 (2023).
[65] M. Buchhold, T. Müller, and S. Diehl, arXiv:2208.10506.
[66] V. Ravindranath, Y. Han, Z.-C. Yang, and X. Chen, Phys. Rev. B **108**, L041103 (2023).
[67] N. O'Dea, A. Morningstar, S. Gopalakrishnan, and V. Khemani, Phys. Rev. B **109**, L020304 (2024).
[68] L. Piroli, Y. Li, R. Vasseur, and A. Nahum, Phys. Rev. B **107**, 224303 (2023).
[69] P. Sierant and X. Turkeshi, Phys. Rev. Lett. **130**, 120402 (2023).
[70] See Supplemental Material at http://link.aps.org/supplemental/10.1103/PhysRevLett.132.163401 for the numerical implementations, additional numerical data, and a qualitative argument for the logarithmic saturation time for the quantum jump evolution, which includes Refs. [71–77].
[71] M. Gross and S. Haroche, Phys. Rep. **93**, 301 (1982).
[72] N. Shammah, S. Ahmed, N. Lambert, S. De Liberato, and F. Nori, Phys. Rev. A **98**, 063815 (2018).
[73] J. I. Latorre, R. Orús, E. Rico, and J. Vidal, Phys. Rev. A **71**, 064101 (2005).
[74] A. Lerose and S. Pappalardi, Phys. Rev. Res. **2**, 012041(R) (2020).
[75] A. Lerose and S. Pappalardi, Phys. Rev. A **102**, 032404 (2020).
[76] R. B. Sidje, ACM Trans. Math. Softw. **24**, 130 (1998).
[77] A. J. Daley, Adv. Phys. **63**, 77 (2014).
[78] G. Ferioli, A. Glicenstein, I. Ferrier-Barbut, and A. Browaeys, arXiv:2207.10361.
[79] F. Iemini, A. Russomanno, J. Keeling, M. Schirò, M. Dalmonte, and R. Fazio, Phys. Rev. Lett. **121**, 035301 (2018).
[80] J. Hannukainen and J. Larson, Phys. Rev. A **98**, 042113 (2018).
[81] F. Carollo, I. Lesanovsky, M. Antezza, and G. De Chiara, arXiv:2306.07330.
[82] A. Cabot, L. S. Muhle, F. Carollo, and I. Lesanovsky, Phys. Rev. A **108**, L041303 (2023).
[83] P. M. Poggi and M. H. Muñoz-Arias, Quantum **8**, 1229 (2024).
[84] This fact holds because the trajectory average does not commute with nonlinear functions of the quantum trajectory [23].

[85] In [70] we present an example of a monitored system having a phase transition at the average level, but lacking a MIPT.

[86] M. Block, Y. Bao, S. Choi, E. Altman, and N. Y. Yao, Phys. Rev. Lett. **128**, 010604 (2022).

[87] S. Sharma, X. Turkeshi, R. Fazio, and M. Dalmonte, SciPost Phys. Core **5**, 023 (2022).

[88] T. Minato, K. Sugimoto, T. Kuwahara, and K. Saito, Phys. Rev. Lett. **128**, 010603 (2022).

[89] T. Müller, S. Diehl, and M. Buchhold, Phys. Rev. Lett. **128**, 010605 (2022).

[90] T. Hashizume, G. Bentsen, and A. J. Daley, Phys. Rev. Res. **4**, 013174 (2022).

[91] P. Zhang, C. Liu, S.-K. Jian, and X. Chen, Quantum **6**, 723 (2022).

[92] N. Gisin and I. C. Percival, J. Phys. A **25**, 5677 (1992).

[93] G. Ferioli (private communication).

[94] Y. Minoguchi, P. Rabl, and M. Buchhold, SciPost Phys. **12**, 009 (2022).

[95] B. Ladewig, S. Diehl, and M. Buchhold, Phys. Rev. Res. **4**, 033001 (2022).

[96] X. Turkeshi, L. Piroli, and M. Schiró, Phys. Rev. B **106**, 024304 (2022).

[97] Z. Weinstein, Y. Bao, and E. Altman, Phys. Rev. Lett. **129**, 080501 (2022).

[98] Z. Weinstein, S. P. Kelly, J. Marino, and E. Altman, Phys. Rev. Lett. **131**, 220404 (2023).

[99] P. Hauke, M. Heyl, L. Tagliacozzo, and P. Zoller, Nat. Phys. **12**, 778 (2016).

[100] L. Pezzè, A. Smerzi, M. K. Oberthaler, R. Schmied, and P. Treutlein, Rev. Mod. Phys. **90**, 035005 (2018).

[101] S. Pappalardi, A. Russomanno, A. Silva, and R. Fazio, J. Stat. Mech. (2017) 053104.

[102] J.-Y. Desaules, F. Pietracaprina, Z. Papić, J. Goold, and S. Pappalardi, Phys. Rev. Lett. **129**, 020601 (2022).

[103] S. Pappalardi, A. Russomanno, B. Žunkovič, F. Iemini, A. Silva, and R. Fazio, Phys. Rev. B **98**, 134303 (2018).

[104] M. Brenes, S. Pappalardi, J. Goold, and A. Silva, Phys. Rev. Lett. **124**, 040605 (2020).

[105] S. Dooley, S. Pappalardi, and J. Goold, Phys. Rev. B **107**, 035123 (2023).

[106] *En passant*, we note that for a pure state $\rho_{\mathrm{w}} = |\Psi\rangle_{\mathrm{w}}\langle\Psi|_{\mathrm{w}}$, $F_Q(\rho_{\mathrm{w}})$ is the maximal eigenvalue of the covariance matrix $M^{\mathrm{cov}}_{\alpha,\beta} = 2\langle\Psi_{\mathrm{w}}|\{\hat{J}_\alpha, \hat{J}_\beta\}|\Psi\rangle - 4\langle\Psi_{\mathrm{w}}|\hat{J}_\alpha|\Psi_{\mathrm{w}}\rangle\langle\Psi_{\mathrm{w}}|\hat{J}_\beta|\Psi_{\mathrm{w}}\rangle$.

[107] We note that in the quantum jump case, the Fisher density is extensive in the system size $\overline{f_Q} \sim N$, cf. Ref. [70].

[108] This fact reveals enhanced multipartite entanglement at the critical point.

[109] A. C. Lourenço, L. F. d. Prazeres, T. O. Maciel, F. Iemini, and E. I. Duzzioni, Phys. Rev. B **105**, 134422 (2022).

[110] F. Iemini and S. Pal (unpublished).

[111] G. Ferioli, A. Glicenstein, F. Robicheaux, R. T. Sutherland, A. Browaeys, and I. Ferrier-Barbut, Phys. Rev. Lett. **127**, 243602 (2021).

[112] N. Roch, M. E. Schwartz, F. Motzoi, C. Macklin, R. Vijay, A. W. Eddins, A. N. Korotkov, K. B. Whaley, M. Sarovar, and I. Siddiqi, Phys. Rev. Lett. **112**, 170501 (2014).

[113] P. Campagne-Ibarcq, P. Six, L. Bretheau, A. Sarlette, M. Mirrahimi, P. Rouchon, and B. Huard, Phys. Rev. X **6**, 011002 (2016).

[114] Nevertheless, no direct relationship is in general present between these variances and the entanglement entropy.

[115] H. Keßler, P. Kongkhambut, C. Georges, L. Mathey, J. G. Cosme, and A. Hemmerich, Phys. Rev. Lett. **127**, 043602 (2021).

[116] Z. Wang, H. Li, W. Feng, X. Song, C. Song, W. Liu, Q. Guo, X. Zhang, H. Dong, D. Zheng, H. Wang, and D.-W. Wang, Phys. Rev. Lett. **124**, 013601 (2020).

[117] C. Liedl, F. Tebbenjohanns, C. Bach, S. Pucher, A. Rauschenbeutel, and P. Schneeweiss, Phys. Rev. X **14**, 011020 (2024).

[118] B. Zhu, J. Marino, N. Y. Yao, M. D. Lukin, and E. A. Demler, New J. Phys. **21**, 073028 (2019).